

Supplementary Material: Generalized Content-Preserving Warps for Image Stitching

BMVC 2018 Submission # 401

This supplementary document consists of three parts. The first part presents the datasets that we use in our experiments. The second part describes the detailed generation process of synthetic images with different degrees of colour variation, which is related to the Section 3.1 of the paper. The third part provides more comparative results with higher image resolution.

1 Datasets



Figure 1: Dataset1 consists of 12 pairs of images. First row: pair 01-06. Second row: pair 07-12. Each pair of images has nearly no colour differences, which are collected from [1, 2, 4]. Dataset1 is used in our synthetic experiments (Section 3.1 of the paper).

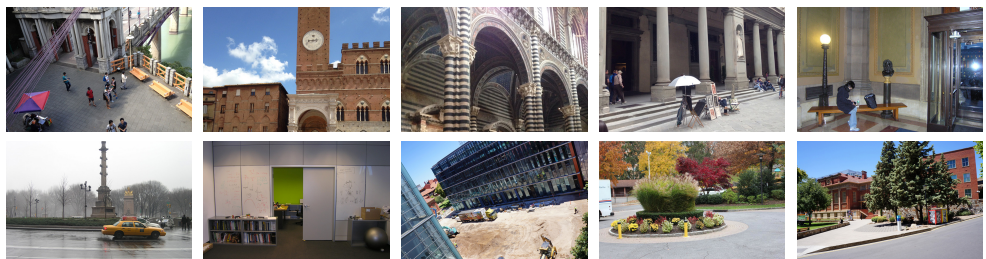


Figure 2: Dataset2 consists of 10 pairs of images. First row: pair 01-05. Second row: pair 06-10. Each pair of images has significant colour differences and are directly collected from [1, 2, 4]. We use Dataset2 to conduct our experiments on real images (Section 3.2 of the paper).

2 Generating Images with Colour Variation

As described in the paper, for each pair of images in the Dataset1, we generate N pairs of images ($N = 16$ in our implementation) with different degrees of colour variations to obtain

our synthetic data. In order to control the degree of colour variation, we adopt the global colour model [3]:

$$I' = (cI)^\gamma, \quad (1)$$

where I is the original image, I' is the synthetic image, c is a scale factor that is related to the white balance ($c = 1.0$ in our implementation) and $(.)^\gamma$ is the non-linear gamma function. In order to create more complex variation that is relevant to spatial positions, we add a spatially-varying factor to the non-linear gamma function and compute the γ of Eq.1 as follows:

$$\gamma = \left(1 + \frac{k-1}{N}\right)^{-a/b} \times \beta, \quad (2)$$

where $k = 1, 2, 3, \dots, N$ denotes the pair index, a is the pixel column coordinate (or row coordinate), b is the image width (or image height). With Eq. 2, we use different values of γ for pixels located on different positions to simulate the local colour variation. We synthesis the colour difference from small to large (k varies from 1 to N) according to the colour model defined by Eq. 1. Specifically, we first convert the source image from RGB colour space to $YCbCr$ colour space. We then conduct colour transformation for each image channel independently. For image Y -channel, we sample the value of β from 1.0 to 0.5. For other two image channels, we sample β from 1.0 to 0.95. Figure 3 presents one group of our synthetic images.

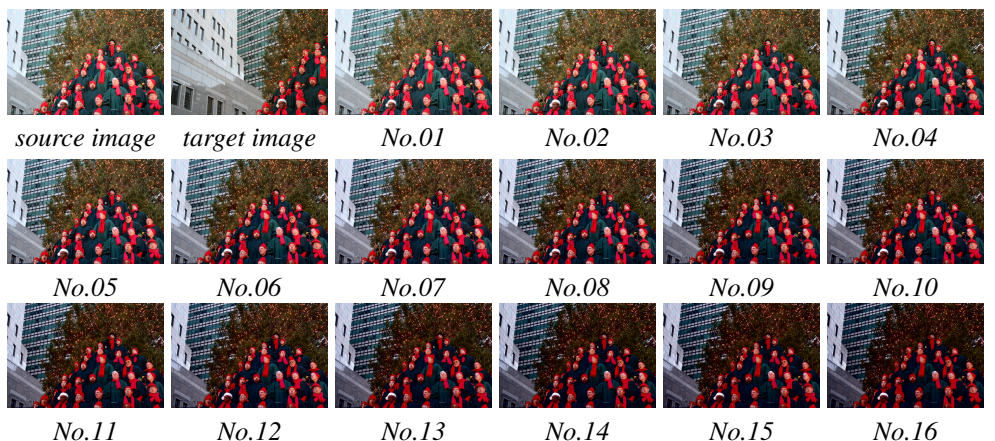


Figure 3: One group of synthetic images generated with our scheme. It consists of 16 pairs of images. We control the colour differences from small to large.

3 Comparative Results

In this part, we present more comparative results with higher image resolution. Specifically, Figure 4 to Figure 9 shows our results on all 12 groups of synthetic images of Dataset1. As for experiments on Dataset2, from Figure 10 to Figure 13, we present the results of our method compared with Global Homography, CPW and DF-W. From Figure 14 to Figure 19, we present the detailed results of our method compared with DF-W, MF-W, LSH+MF-W and ROS+MF-W.

092 References

- 093
- 094 [1] Yu-Sheng Chen and Yung-Yu Chuang. Natural image stitching with the global similarity
095 prior. In *European Conference on Computer Vision (ECCV)*, pages 186–201, 2016.
- 096 [2] Shiwei Li, Lu Yuan, Jian Sun, and Long Quan. Dual-feature warping-based motion
097 model estimation. In *IEEE International Conference on Computer Vision (ICCV)*, pages
098 4283–4291, 2015.
- 099
- 100 [3] Jaesik Park, Yu-Wing Tai, Sudipta N Sinha, and In So Kweon. Efficient and robust color
101 consistency for community photo collections. In *IEEE Conference on Computer Vision
102 and Pattern Recognition (CVPR)*, pages 430–438, 2016.
- 103 [4] Julio Zaragoza, Tat-Jun Chin, Michael S Brown, and David Suter. As-projective-as-
104 possible image stitching with moving dlt. In *IEEE Conference on Computer Vision and
105 Pattern Recognition (CVPR)*, pages 2339–2346, 2013.
- 106
- 107
- 108
- 109
- 110
- 111
- 112
- 113
- 114
- 115
- 116
- 117
- 118
- 119
- 120
- 121
- 122
- 123
- 124
- 125
- 126
- 127
- 128
- 129
- 130
- 131
- 132
- 133
- 134
- 135
- 136
- 137

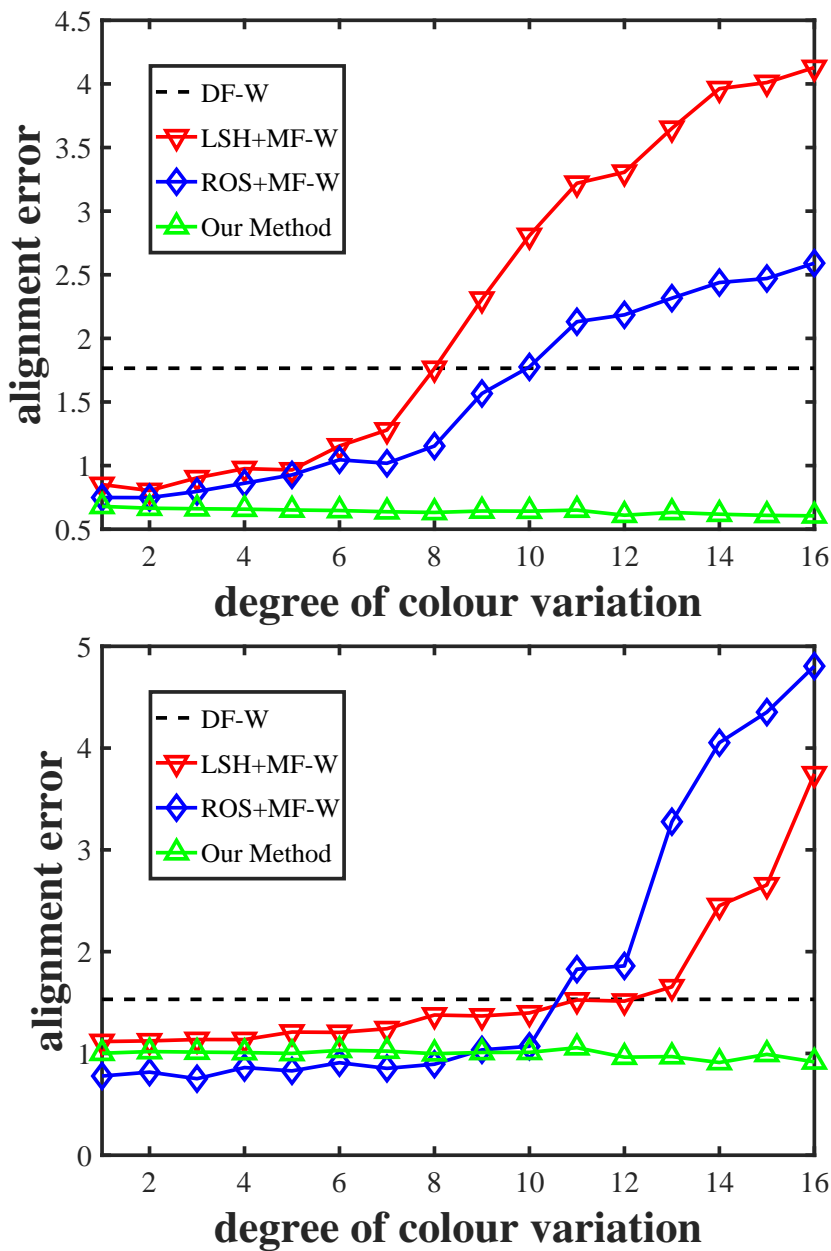


Figure 4: Comparative results on image pair 01-02.

138
139
140
141
142
143
144
145
146
147
148
149
150
151
152
153
154
155
156
157
158
159
160
161
162
163
164
165
166
167
168
169
170
171
172
173
174
175
176
177
178
179
180
181
182
183

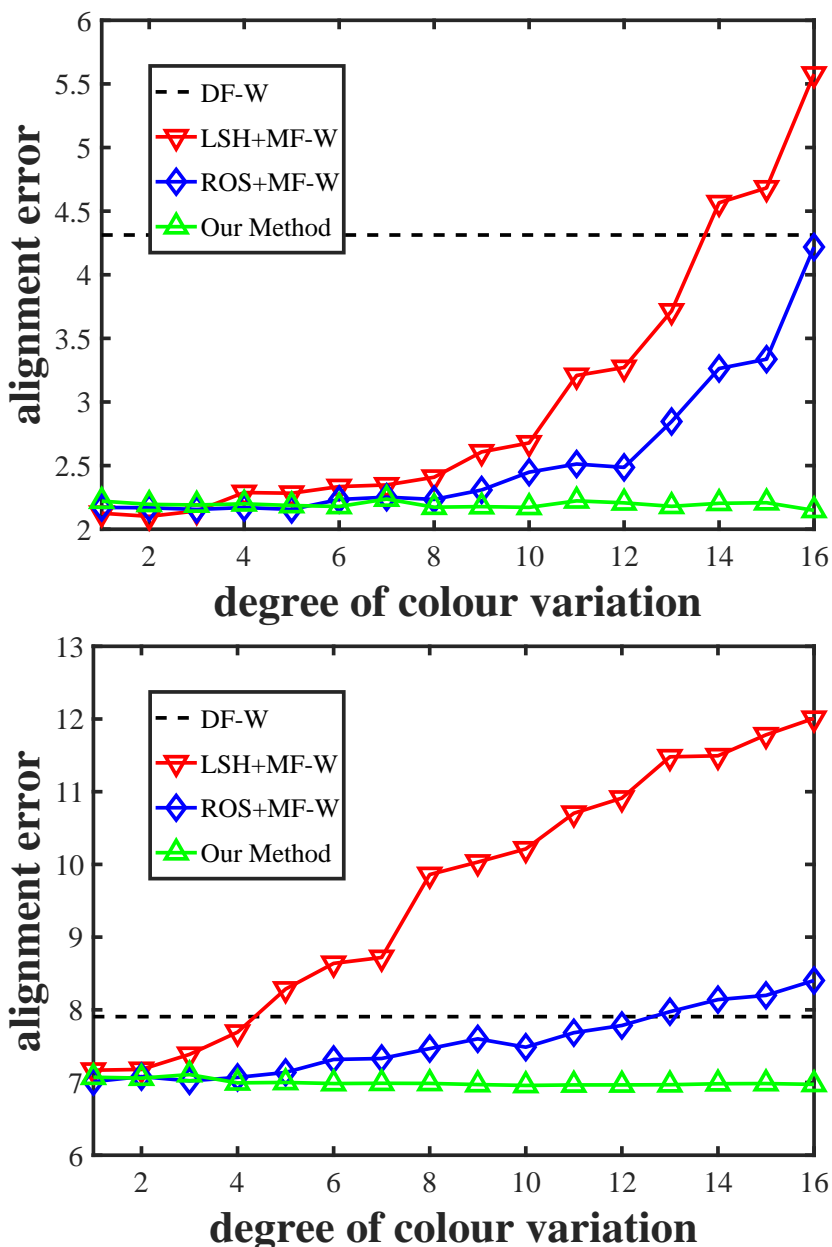


Figure 5: Comparative results on image pair 03-04.

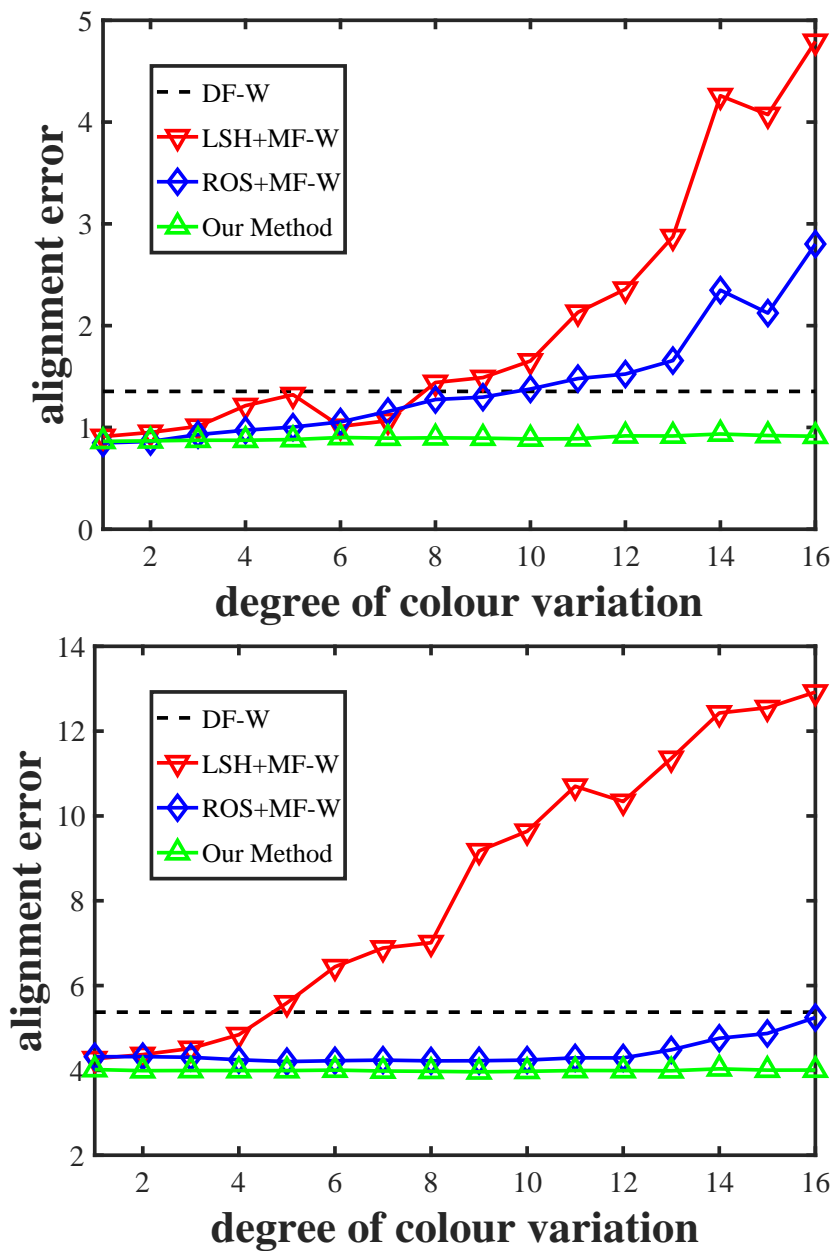
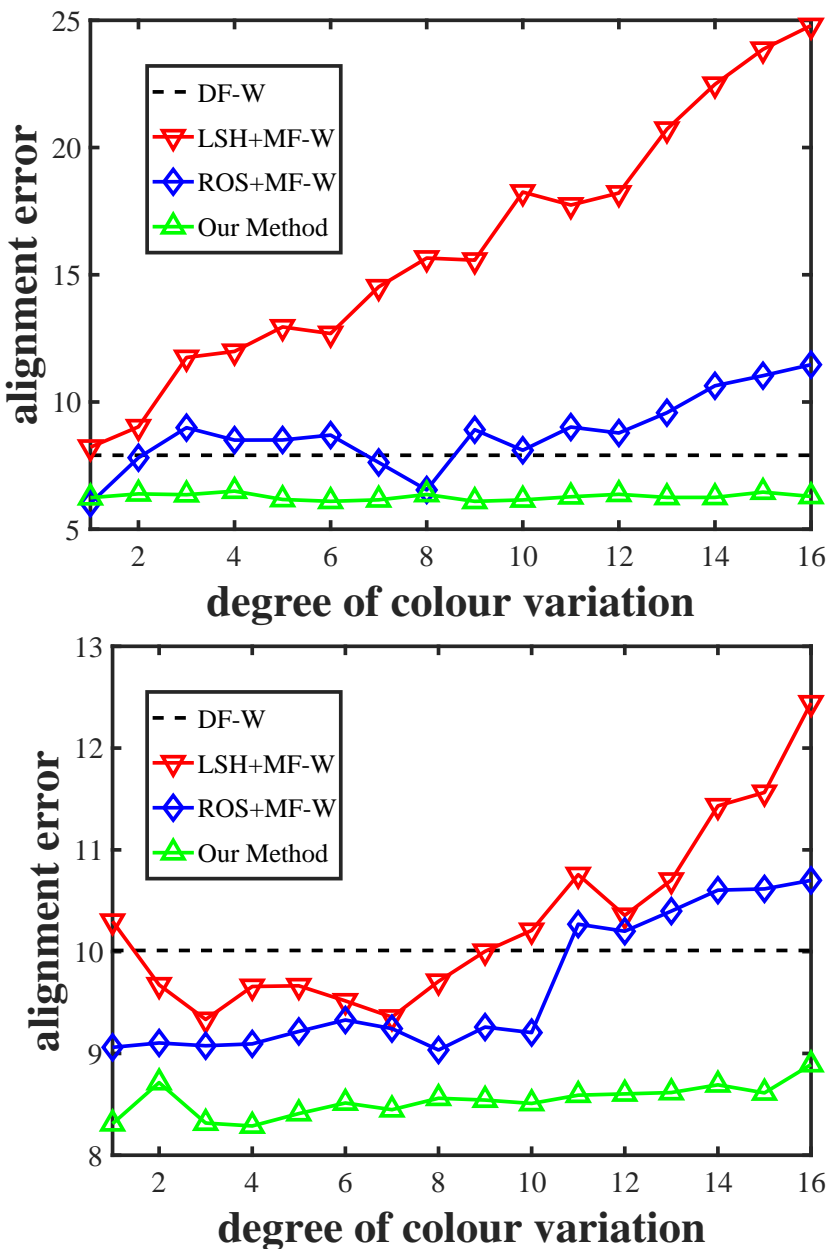


Figure 6: Comparative results on image pair 05-06.

230
231
232
233
234
235
236
237
238
239
240
241
242
243
244
245
246
247
248
249
250
251
252
253
254
255
256
257
258
259
260
261
262
263
264
265
266
267
268
269
270
271
272
273
274
275

317
318 Figure 7: Comparative results on image pair 07-08.
319
320
321

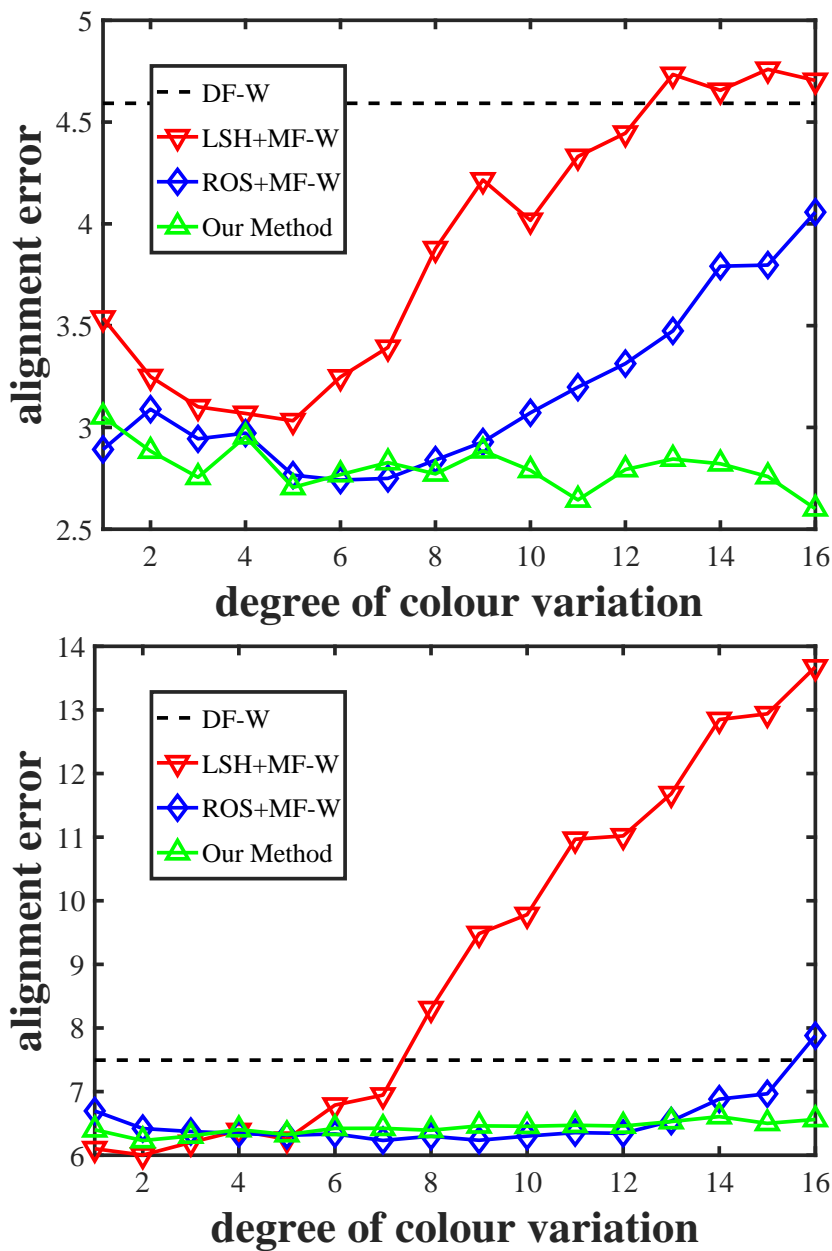


Figure 8: Comparative results on image pair 09-10.

322
323
324
325
326
327
328
329
330
331
332
333
334
335
336
337
338
339
340
341
342
343
344
345
346
347
348
349
350
351
352
353
354
355
356
357
358
359
360
361
362
363
364
365
366
367

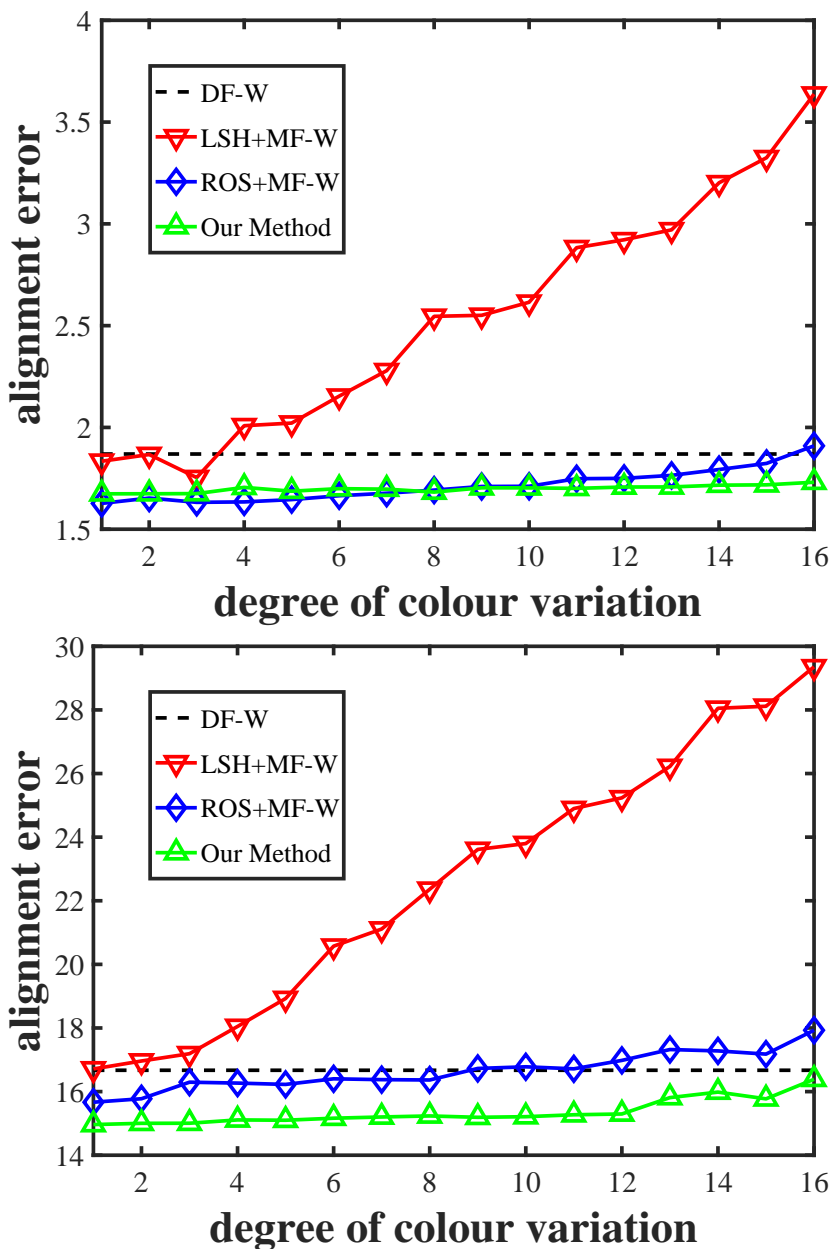
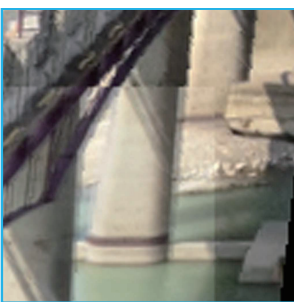
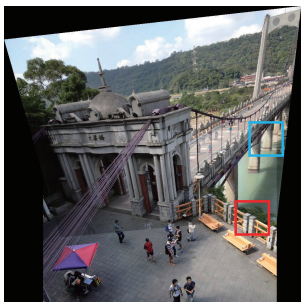
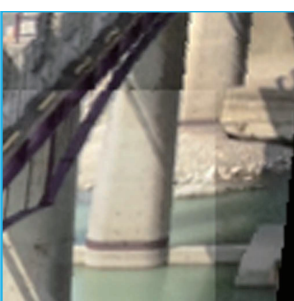
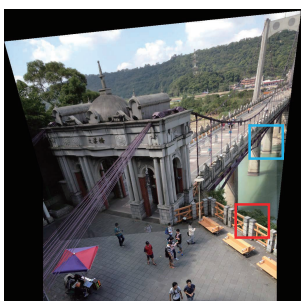


Figure 9: Comparative results on image pair 11-12.

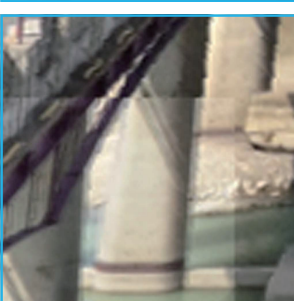
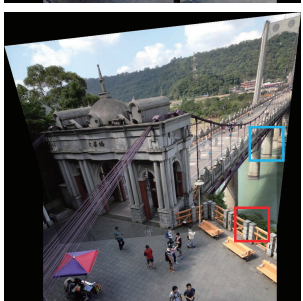
Global



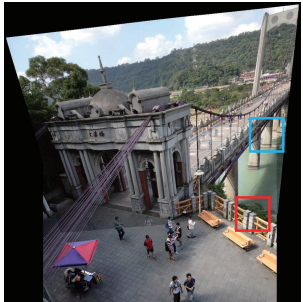
CPW



DF-W



Ours



414

415

416

417

418

419

420

421

422

423

424

425

426

427

428

429

430

431

432

433

434

435

436

437

438

439

440

441

442

443

444

445

446

447

448

449

450

451

452

453

454

455

456

457

458

459

Figure 10: Comparisons with Global Homography, CPW and DF-W: Image pair 01.

460
461
462
463
464
465
466
467
468
469
470
471
472
473
474
475
476
477
478
479
480
481
482
483
484
485
486
487
488
489
490
491
492
493
494
495
496
497
498
499
500
501
502
503
504
505

Global
CPW
DF-W
Ours

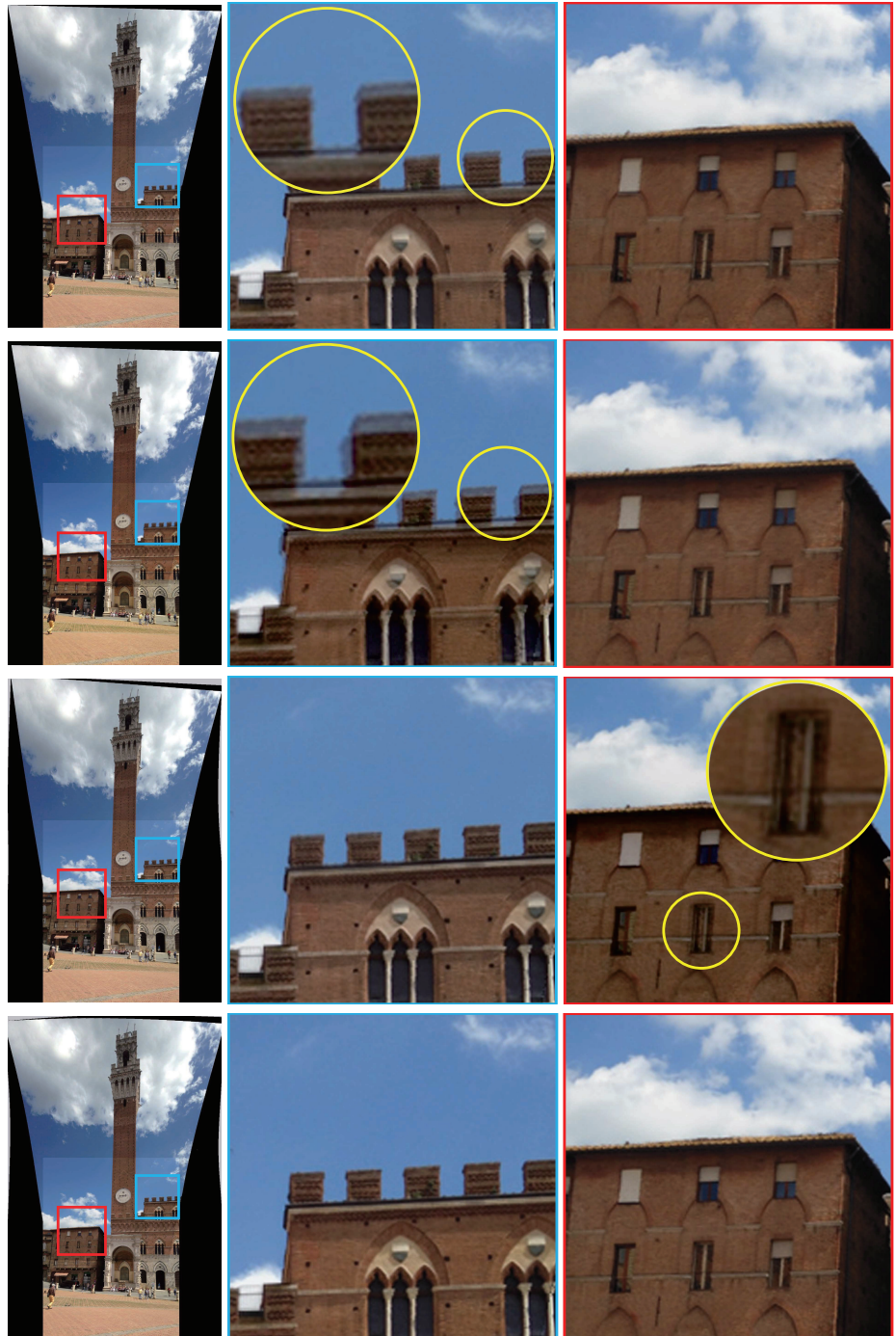
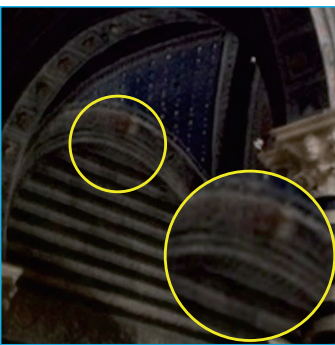
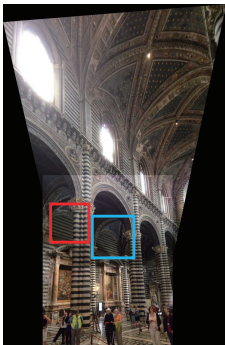
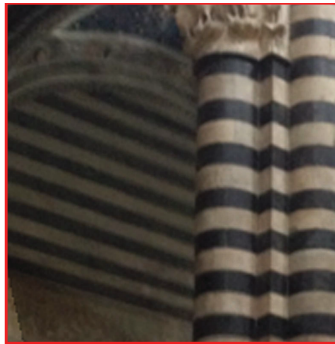
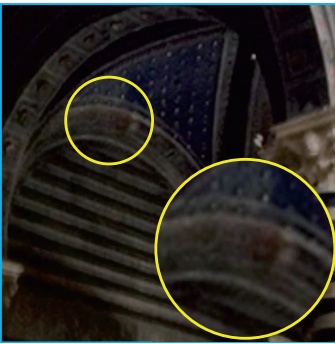
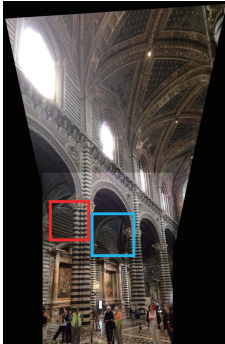


Figure 11: Comparisons with Global Homography, CPW and DF-W: Image pair 02.

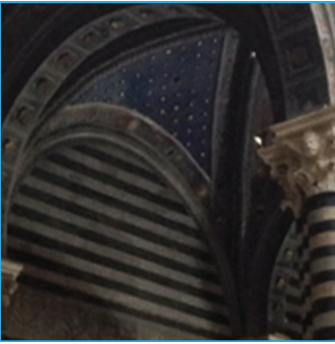
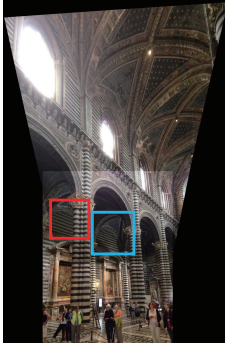
Global



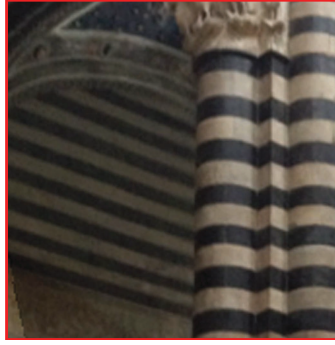
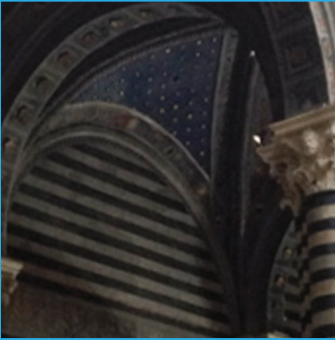
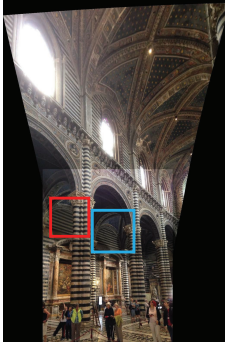
CPW



DF-W



Ours



506
507
508
509
510
511
512
513
514
515
516
517
518
519
520
521
522
523
524
525
526
527
528
529
530
531
532
533
534
535
536
537
538
539
540
541
542
543
544
545
546
547
548
549
550
551

Figure 12: Comparisons with Global Homography, CPW and DF-W: Image pair 03.

552

553

554

555

556

557

558

559

560

561

562

563

564

565

566

567

568

569

570

571

572

573

574

575

576

577

578

579

580

581

582

583

584

585

586

587

588

589

590

591

592

593

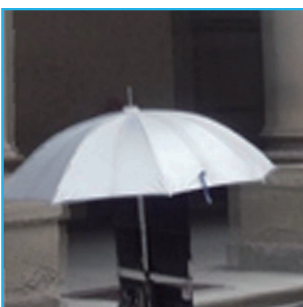
594

595

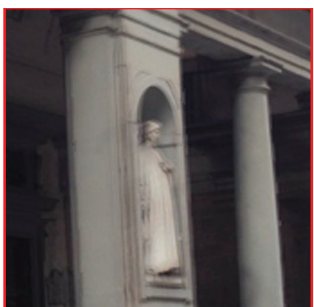
596

597

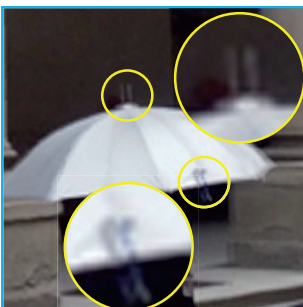
Global



CPW



DF-W



Ours

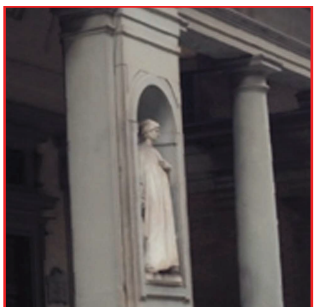
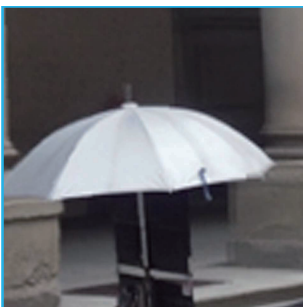


Figure 13: Comparisons with Global Homography, CPW and DF-W: Image pair 04.

DF-W



MF-W



LSH+MF-W



ROS+MF-W



Ours



Figure 14: Comparisons with DF-W, MF-W, LSH+MF-W and ROS+MF-W: Image pair 05.

598
599
600
601
602
603
604
605
606
607
608
609
610
611
612
613
614
615
616
617
618
619
620
621
622
623
624
625
626
627
628
629
630
631
632
633
634
635
636
637
638
639
640
641
642
643

644

645

646

647

648

649

650

651

652

653

654

655

656

657

658

659

660

661

662

663

664

665

666

667

668

669

670

671

672

673

674

675

676

677

678

679

680

681

682

683

684

685

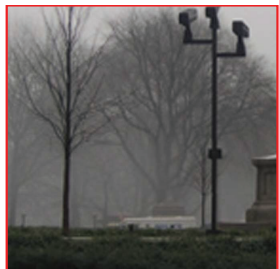
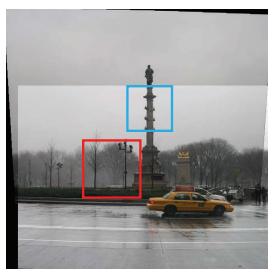
686

687

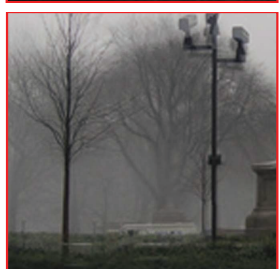
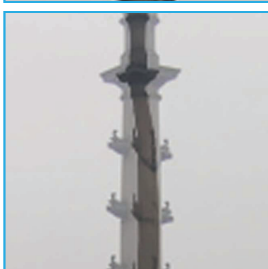
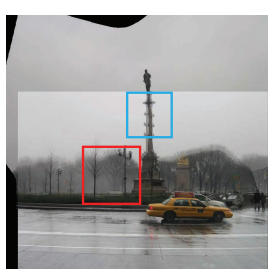
688

689

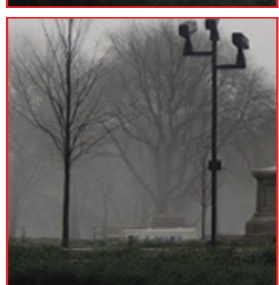
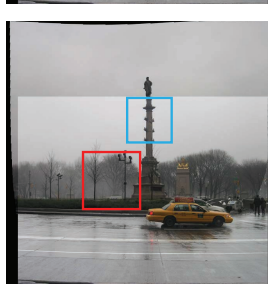
DF-W



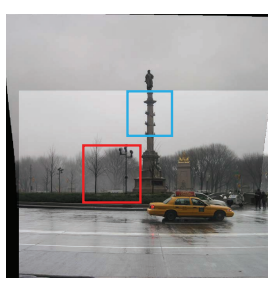
MF-W



LSH+MF-W



ROS+MF-W



Ours

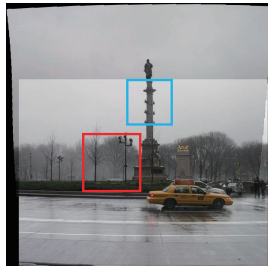
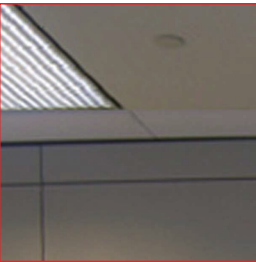
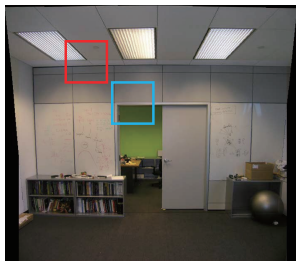
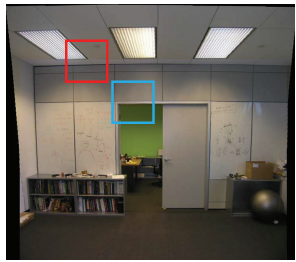


Figure 15: Comparisons with DF-W, MF-W, LSH+MF-W and ROS+MF-W:
Image pair 06.

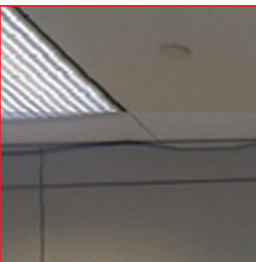
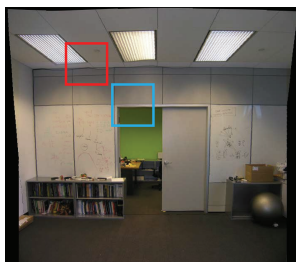
DF-W



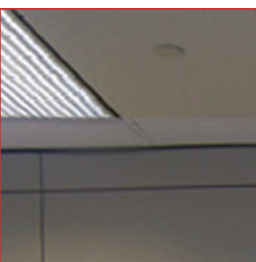
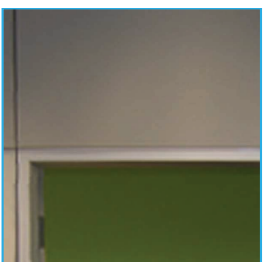
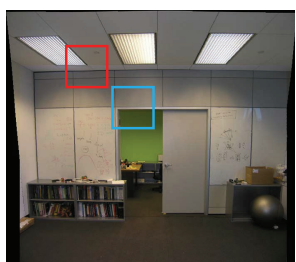
MF-W



LSH+MF-W



ROS+MF-W



Ours

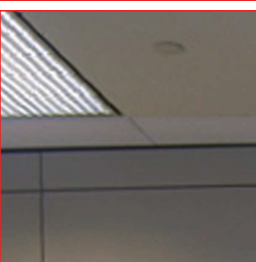
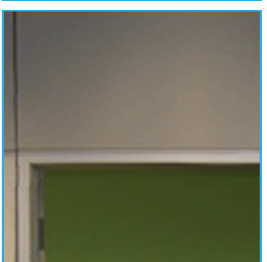
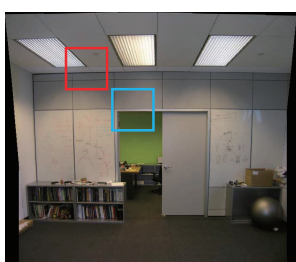


Figure 16: Comparisons with DF-W, MF-W, LSH+MF-W and ROS+MF-W:
Image pair 07.

690
691
692
693
694
695
696
697
698
699
700
701
702
703
704
705
706
707
708
709
710
711
712
713
714
715
716
717
718
719
720
721
722
723
724
725
726
727
728
729
730
731
732
733
734
735

736

737

738

739

740

741

742

743

744

745

746

747

748

749

750

751

752

753

754

755

756

757

758

759

760

761

762

763

764

765

766

767

768

769

770

771

772

773

774

775

776

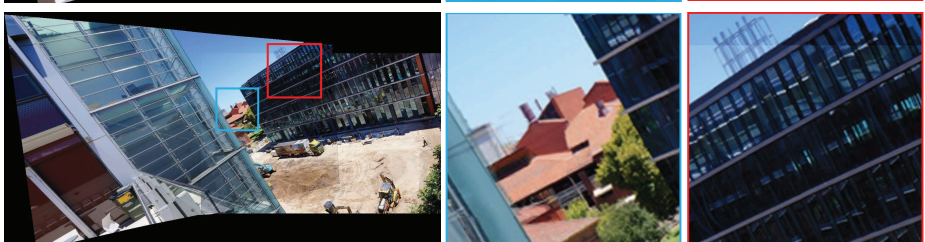
DF-W



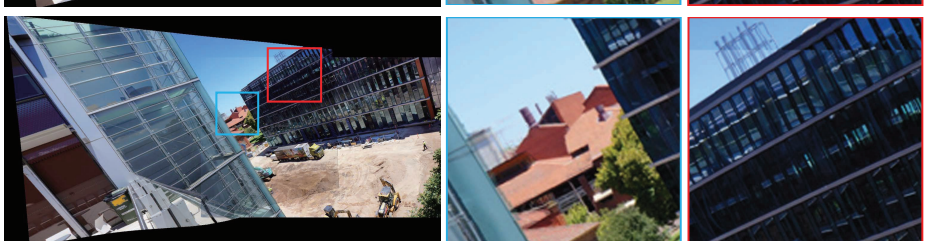
MF-W



LSH+MF-W



ROS+MF-W



Ours

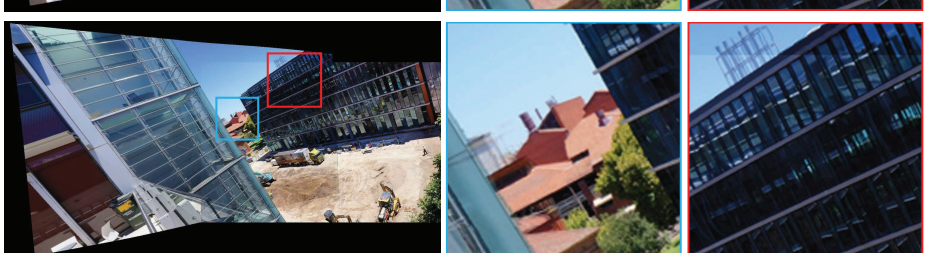


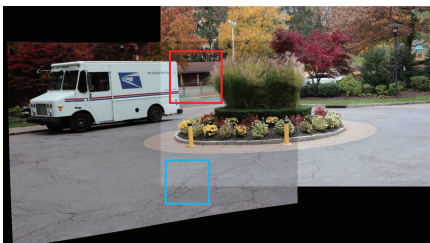
Figure 17: Comparisons with DF-W, MF-W, LSH+MF-W and ROS+MF-W: Image pair 08.

779

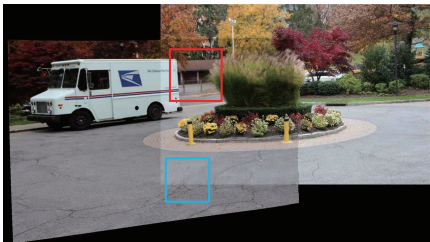
780

781

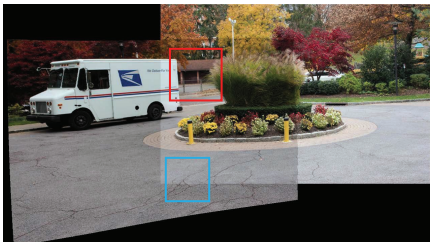
DF-W



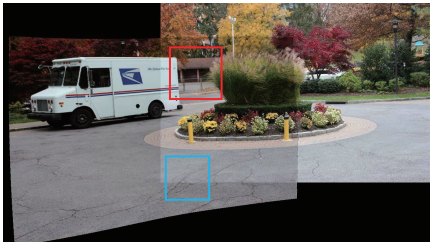
MF-W



LSH+MF-W



ROS+MF-W



Ours

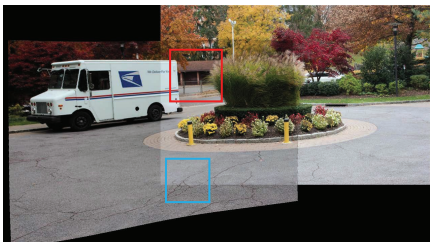


Figure 18: Comparisons with DF-W, MF-W, LSH+MF-W and ROS+MF-W: Image pair 09.

782

783

784

785

786

787

788

789

790

791

792

793

794

795

796

797

798

799

800

801

802

803

804

805

806

807

808

809

810

811

812

813

814

815

816

817

818

819

820

821

822

823

824

825

826

827

828

829

830

831

832

833

834

835

836

837

838

839

840

841

842

843

844

845

846

847

848

849

850

851

852

853

854

855

856

857

858

859

860

861

862

863

864

865

866

867

868

869

870

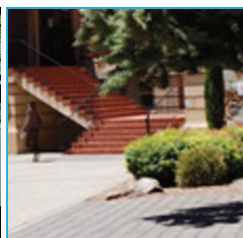
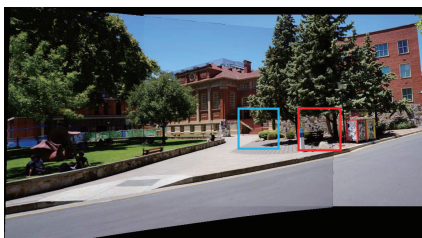
10.

871

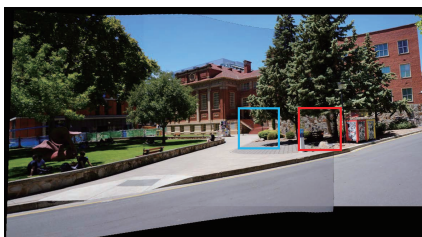
872

873

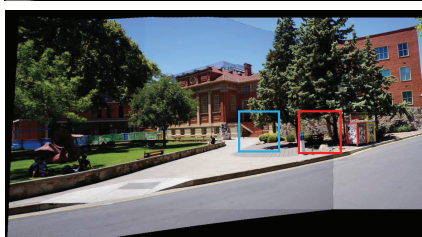
DF-W



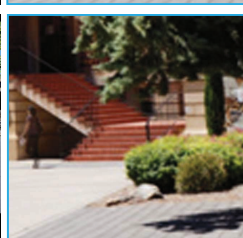
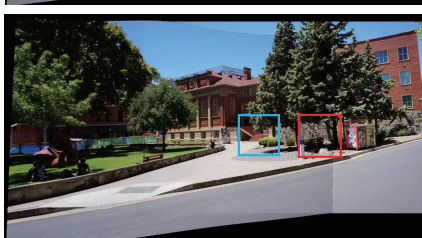
MF-W



LSH+MF-W



ROS+MF-W



Ours

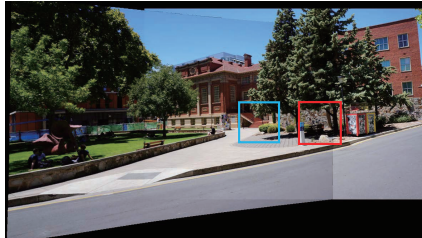


Figure 19: Comparisons with DF-W, MF-W, LSH+MF-W and ROS+MF-W: Image pair 10.